Optimization of operating parameters for xylose reductase separation through ultrafiltration membrane using response surface methodology

Santhana Krishnan[a,*], B. Noor Suzana[b], Zularisam Abdul Wahid[c], Mohd Nasrullah[c], Mimi Sakinah Abdul Munaim[b,c,**], Mohd Fadhil Bin MD Din[a], Shazwin Mat Taib[d], Yu You Li[e]

[a] Center of Environmental Sustainability and Water Security (IPASA), Research Institute of Sustainable Environment (RISE), School of Civil Engineering, Faculty of Engineering, Universiti Teknologi Malaysia (UTM), 81310, Johor Bahru, Malaysia
[b] Faculty of Chemical Engineering and Natural Resources, Universiti Malaysia Pahang, Lebuhraya Tun Razak, 26300, Kuantan Pahang, Malaysia
[c] Faculty of Civil Engineering Technology, Universiti Malaysia Pahang, Lebuhraya Tun Razak, 26300, Kuantan, Pahang, Malaysia
[d] Center for Coastal and Ocean Engineering, Research Institute for Sustainable Environment, Universiti Teknologi Malaysia, Jalan Sultan Yahya Petra, 54100, Kuala Lumpur, Malaysia
[e] Department of Civil and Environmental Engineering, Graduate School of Engineering, Tohoku University, Aoba-ku, Sendai, 980-8579, Japan

ARTICLE INFO

ABSTRACT

The application of the xylose reductase (XR) enzyme in the development of biotechnology demands an efficient and large scale enzyme separation technique. The aim of this present work was to optimize xylose reductase (XR) purification process through ultrafiltration membrane (UF) technology using Central composite design (CCD) of response surface methods (RSM). The three effective parameters analyzed were filtration time (0–100), transmembrane pressure (TMP) (1–1.6 bar), cross flow velocity (CFV) (0.52–1.2 cm/s^{-1}) and its combined effect to obtain high flux with less possibility of membrane fouling. Experimental studies revealed that the best range for optimization process for filtration time, operational transmembrane pressure and cross flow velocity was 30 min, 1.4 bars and 1.06 cm/s, respectively as these conditions yielded the highest membrane permeability (56.03 $Lm^{-2}h^{-1} bar^{-1}$) and xylitol content (15.49 g/l). According to the analysis of variance (ANOVA), the p-value (<0.0001) indicated the designed model was highly significant. The error percentage between the actual and predicted value for membrane permeability and xylitol amount (2.21 % and 4.85 % respectively), which both were found to be close to the predicted values. The verification experiments gave membrane actual permeability of 57.3 $Lm^{-2}h^{-1} bar^{-1}$ and 16.29 g/l of xylitol production, thus indicating that the successfully developed model to predict the response.

1. Introduction

Recent biotechnology advances have opened up new avenues for the production of essential biomolecules such as enzymes and proteins [1]. While a considerable amount of work has been carried out in this area, the technology to separate biological products from reaction mixtures has not kept up with advances in upstream processing [2]. Given the recognized fact that downstream processing accounts for a large share of the final product costing, there has been a growing interest in the discovery of efficient downstream processing methods for the separation, concentration and purification of biomolecules [3].

Xylose reductase (XR) is one of the key enzymes for xylitol production, therefore understanding the mechanisms that regulate its activity could help to establish the optimal process conditions of separating XR [4]. XR was the first enzyme used in the D- xylose isomerization pathway, where it has shown to control the rate of D-xylose utilization and therefore the enzyme application demands an efficient and large scale enzyme separation technique [5]. The techniques that are routinely used in laboratories (e.g. chromatography or affinity purification) can be employed for enzyme separation [6], but they are only suitable for producing small quantities of the enzyme. Moreover, such techniques not only require complex instrumentations but also have low production efficiency and high cost [7].

* Corresponding author.
** Corresponding author at: Center of Environmental Sustainability and Water Security (IPASA), Research Institute of Sustainable Environment (RISE), School of Civil Engineering, Faculty of Engineering, Universiti Teknologi Malaysia (UTM), 81310, Johor Bahru, Malaysia.
E-mail addresses: kcsanthana@utm.my (S. Krishnan), mimi@ump.edu.my (M.S. Abdul Munaim).

Membranes have become an integral part of biotechnology and improvements in membrane technology are now focused on achieving higher resolutions of the bioproduct [8]. Membrane technology are increasingly employed for various applications in both upstream and downstream technologies, such as microfiltration (MF), ultrafiltration (UF), emerging processes such as membrane chromatography, high performance tangential flow filtration, and electrophoretic membrane contactor [9]. Membrane-based processes are playing a critical role in the field of separation/purification of biotechnological products which include protein production/purification and protein–virus separation [10]. Morthensen et al., developed an integrated system of cofactor regeneration and xylose purification using membrane reactor equipped with charged nanofiltration (NF) membrane. The product was separated based on charge repulsion and size exclusion in a sequence of two NF steps [11]. As advancements are made in the membrane production and module design, the capital and operating costs continue to decline [12]. Among the membrane process, the UF process is a cost-effective method that gives high productivity and reasonable product purity. The process is also easier to scale-up compared to the chromatography and other electrophoresis techniques. The UF process seems to be less expensive, isothermal, and easy to scale-up, has the advantages of ensuring high values of products, preserving the targeted biomolecules, and yielding satisfactory separation performance [13]. Zaccaria et al., investigated the use of ultrafiltration membranes for the concentration of laccase-rich enzymatic extract of *Pleurotus sajor-caju* PS-2001. Concentration by ultrafiltration resulted in a superior recovery percentage of 141 %, but under low permeate flow 20 L m^{-2} h^{-1} and longer process time with laccase activity of ca. 3033 U mL^{-1} [14].

Operating conditions such as transmembrane pressure (TMP) and cross-flow velocity (CFV) have an effect on the purification performance and fouling phenomenon [15]. Hence its optimization of such critical factors are very important for high product yields. High cross-flow velocity induces turbulence, reduces concentration polarization and increases shear stress in the laminar region. Although TMP is the driving force for permeation, the flux increases with pressure up to a limiting value (TMP$_{lim}$), which depends on the physical properties of the suspension to be filtered and on the CFV [16]. At higher TMP, the flux becomes independent of pressure due to concentration polarization. For optimal flux, a TMP at the point at which flux levels off is usually chosen. Among the multivariate statistic methods, response surface methodology (RSM) is one of the relevant multi-variant techniques which can deal with multi-variant experimental design strategy, statistical modelling, and process optimization [17]. This method is often employed after the important controllable factors are identified and to find the factor that optimizes the response [18]. The conventional method that has been widely applied is known as one factor at one time (OFAT). The statically experimental design also could determine the interactions between factors that might be revealed in the employed experimental data [19]. Optimization of multiple factors using RSM has proved to be a suitable tool, but its application in the Xylose reductase is still not yet explored.

Therefore, this research is focused on studying the separation of XR from product mixtures using an ultrafiltration membrane. The RSM study was applied in the separation process, in which filtration time, transmembrane pressure and cross flow velocity was optimized as it is important to obtain high flux with less possibility of membrane fouling. This study helps to minimize the production cost for xylitol production.

2. Materials and methods

2.1. Characterization of ultrafiltration membrane

The membrane cassette was purchased from GE Healthcare Biosciences Corp, Piscataway, USA. The commercial ultrafiltration membrane was made from polyethersulfone with the molecular cut-off (MWCO) and membrane effective area of 10 kDa and 0.11 m^2, respectively. It was dried at room temperature for three days before analyzing with FTIR. Infrared measurements were recorded using an attenuated Perkin Elmer (Spectrum 100) FTIR spectroscopy using attenuated total reflection (ATR) mode in ZnSc crystal, over range of 500-4000 cm^{-1}. The spectrum of the membrane was analyzed using the OMNIC software [20].

2.2. One Factor at One-Time Approach (OFAT) approach

The feed mixtures for the UF membrane process has been formulated according to Rafiqul, et al., [21]. The concentration of xylitol, xylose, glucose, arabinose, acetic acid and XR was 16.28 g/l, 2.52 g/l, 4.64 g/l, 2.55 g/l, 3.2 g/l and 0.94 g/l respectively. The mixtures were continuously subjected into the filtration process using an ultrafiltration cassette membrane. Filtration process were run at 1.2 bar and 1.06 cm/s in order to study the effects of the filtration time. The pure water flux (J_{pwp}) was measured by taking the volume of permeates in every 10 min during the preliminary filtration stage. After that, deionized water was replaced with the simulated mixtures and the permeates were collected every 10 min until the flux reached a steady state and measured. The effects of TMP was performed at 0.8, 1.0,1.2,1.4 and 1.6 bar with the constant CFV of 1.06 cm/s. CFV was varied at 0.58, 0.70, 0.88, 1.06 and 1.24 cm/s at a constant TMP (1.2 bar), to determine the effects of CFV. The adjustable feed valve was used to increase the pressure at a rate of 0.2 bar for every 10 min and the flux was recorded by collecting the permeate every 5 min. On other hand, the CFV was controlled by optimizing the feed velocity at a rate of 0.5 cm/min into the membrane. Finally, the flux was recorded by collecting the permeate everyb5 min [20].

2.3. Optimization using Central Composite Design (CCD)

Central composite design (CCD) was used for the optimization process in order to determine the optimum levels of various factors with the interrelations between each factors evolved simultaneously [22]. The design was consisted of a 2^k factorial design augmented by 2k axial (star) points and n$_0$ center points, where α is the distance of the star point from the center. The axial distance was chosen as 2.0 to make this design rotatable. For predicting the optimal point, a second – order polynomial function (Eq. (1)) was fitted to the experimental result.

$$Y = \beta_o + \sum_{i=1}^{k} \beta_i x_i + \sum_{i=1}^{k} \beta_{ii} x_i^2 + \sum \sum_{i<j}^{k} \beta_{ij} x_i x_j \qquad (1)$$

where Y is the predicted response, β$_0$ is the offset term, β_i is the linear effect, β_{ii} is the squared effect, and β$_{ij}$ is the interaction effect. The quality of the fit of the second- order polynomial model equation is expressed by the coefficient of determination R^2, and its statistical significance is checked by F- test. The F–test was used to evaluate the significance of the model. Table 1 shows the factors and levels for the optimization of the operating parameters during the separation of XR.

Table 1
Factors and levels for the central composite design (CCD).

| Variables	Symbols		Levels				
	Coded	Actual	−2	−1	0	1	+2
Filtration time, (min)	X_1	x_1	20	40	60	80	100
TMP, (bar)	X_2	x_2	0.8	1.0	1.2	1.4	1.6
CFV, (cm/s^{-1})	X_3	x_3	0.52	0.70	0.82	1.06	1.20
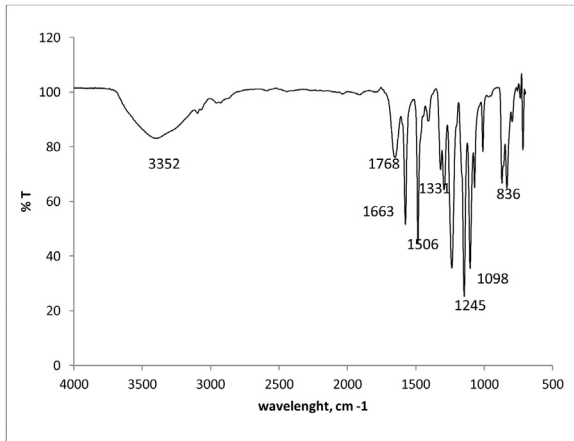
Fig. 1. FTIR spectra of UF membrane.
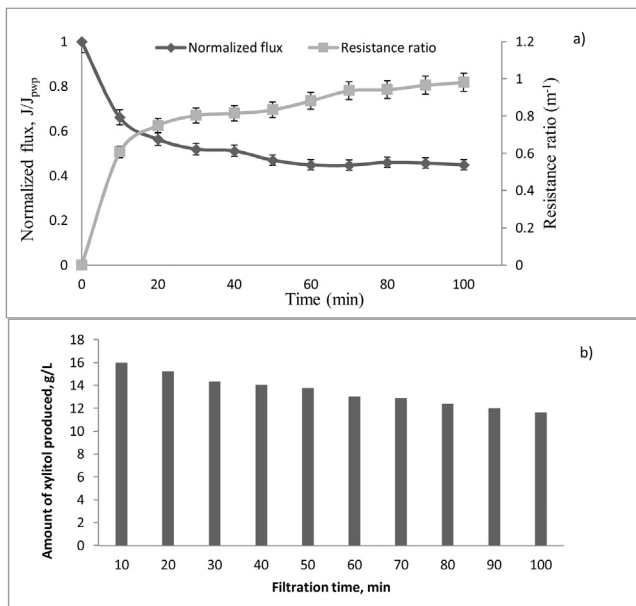
Fig. 2. Effect of Filtration Time. (a) Normalized flux and resistance ratio profile as function of filtration time. (b) Amount of xylitol during 100 min of filtration.

2.4. Calculations

The membrane intrinsic resistance (R_m) was determined by using Darcy's law Equation as given below

$$\frac{J_{pwp}}{\Delta \Pi} = \frac{1}{\mu R_m} \qquad (2)$$

where μ is the dynamic viscosity of water and $J_{pwp}/\Delta P$ is the graph's slope.
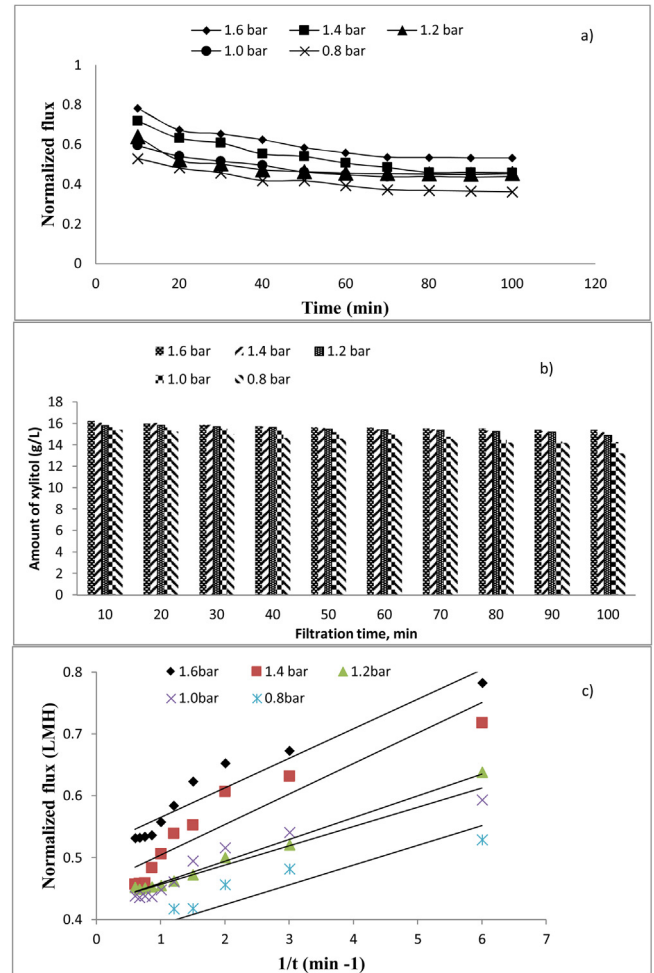
Fig. 3. (a) Effect of transmembrane pressure on membrane flux. (b) Effect of amount xylitol produced at different pressure (c) Fouling Model.

The hydraulic resistance of the membrane (r_m) was evaluated using below equation

$$J = Q = \frac{\Delta \Pi}{A} \, r_{m-} \qquad (3)$$

where J is the flux through the membrane (LMH), ΔP is the transmembrane pressure (Pa), μ is the dynamic viscosity (Pa hr) and r_m is the membrane hydraulic resistance (m^{-1}). The membrane intrinsic resistance (R_m) in this study was found to be 1.10×10^{12} m^{-1}.

2.5. Analytical methods

The concentrations of xylose, glucose, arabinose, xylitol and acetic acid was determined by high performance liquid chromatography (HPLC) using an Agilent 1200 chromatograph (Agilent, USA) equipped with a Refractive Index detector (RID). Ultrapure water was used as mobile phase at a flow rate of 0.6 mL/min and 20 μL of filtered sample was injected by auto sampler. The mobile phase was previously vacuum filtered using 0.45 μm nylon membrane filter and degassed in an ultrasonic bath for 60 min to remove any dissolved air [21]. The XR activity was determined
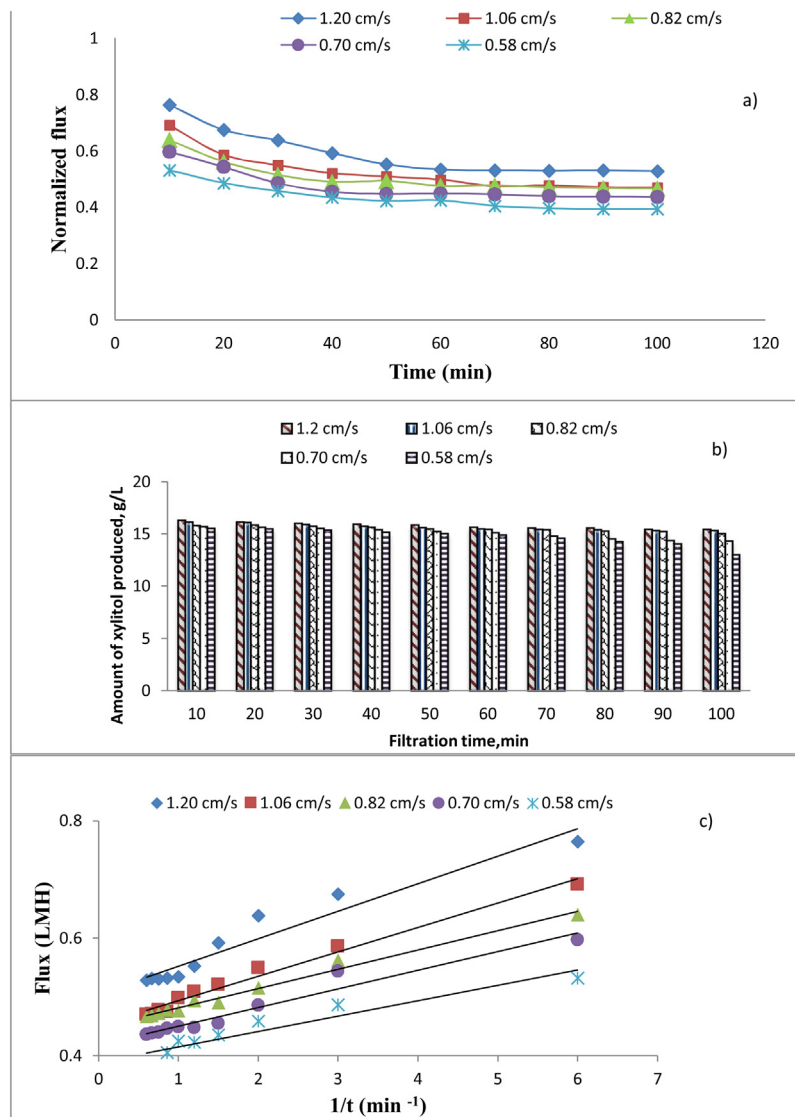
Fig. 4. Effect of crossflow velocity on membrane flux (a) Determination of fouling coefficient (a) at different pressure, (b) at different cross flow velocity, (c) Fouling model.

Table 2
Experimental design and results (actual and predicted values) of the full factorial central composite design.

Std Run	Time (min)	TMP (bar)	CFV (cm/s)	Membrane permeability (L m^{-1} h^{-1} bar^{-1})		Amount of xylitol (g/L)	
				Actual	Predicted	Actual	Predicted
1	30.00	1.00	0.70	50.20	50.31	15.09	15.03
2	50.00	1.00	0.70	48.32	48.48	13.90	13.86
3	30.00	1.40	0.70	51.86	51.97	15.87	15.84
4	50.00	1.40	0.70	49.87	49.90	15.30	15.38
5	30.00	1.00	1.06	52.40	52.53	16.17	16.07
6	50.00	1.00	1.06	50.34	50.39	15.33	15.34
7	30.00	1.40	1.06	57.30	57.30	16.26	16.28
8	50.00	1.40	1.06	54.85	54.91	16.21	16.25
9	20.00	1.20	0.88	54.50	54.41	16.18	16.26
10	60.00	1.20	0.88	50.25	50.19	15.12	15.07
11	40.00	0.80	0.88	47.43	47.29	14.31	14.40
12	40.00	1.60	0.88	53.49	53.47	16.18	16.12
13	40.00	1.20	0.52	49.65	49.53	14.32	14.34
14	40.00	1.20	1.24	56.80	56.76	16.25	16.26
15	40.00	1.20	0.88	51.87	52.07	15.67	15.80
16	40.00	1.20	0.88	52.17	52.07	15.53	15.80
17	40.00	1.20	0.88	51.84	52.07	15.72	15.80
18	40.00	1.20	0.88	52.50	52.07	16.00	15.80
19	40.00	1.20	0.88	52.27	52.07	15.98	15.80
20	40.00	1.20	0.88	51.93	52.07	15.89	15.80

a)

d)

b)

e)

c)

f)
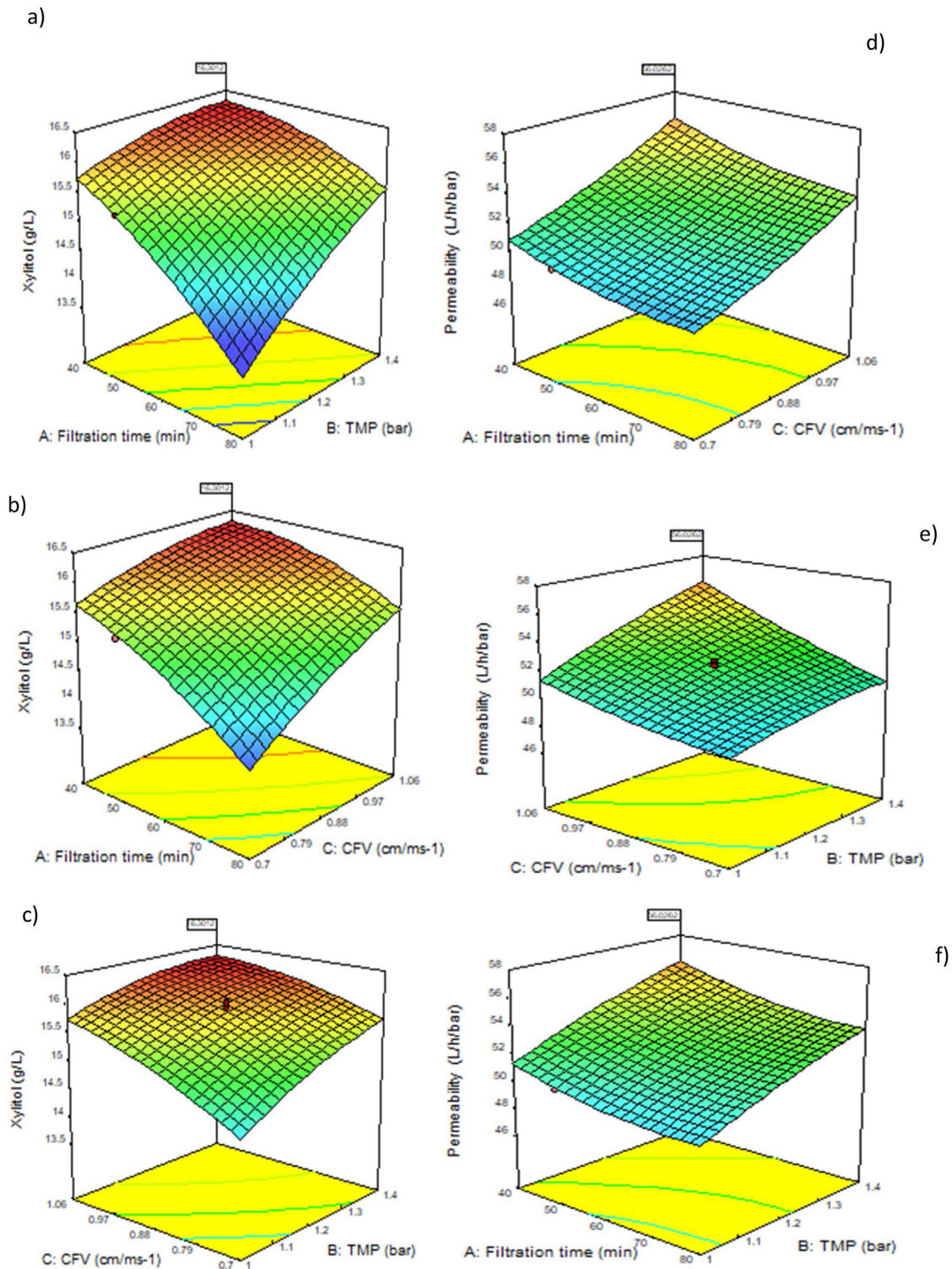
Fig. 5. Response surface plots for the membrane permeability (a-c) and, amount of xylitol produced with reference to each variable (d-f).

spectrophotometrically at 340 nm by monitoring the oxidation of NADPH in a quartz cuvette (1 cm path length) at 25 °C. The reaction mixture in the cuvette (3.5 mL) contained 0.2 mL of 0.1 M potassium phosphate buffer (pH 7.0), 0.2 mL of 0.1 M 2-mercaptoethanol, 0.1 mL XR, 0.1 mL of 3.4 mM NADPH and 1.2 mL of sterile ultrapure water. The reaction was initiated by adding the 0.2 mL of 0.5 M D-xylose.

3. Results and discussion

3.1. FTIR characterization

FTIR spectrum analysis of the membrane was carried out to identify the types of functional groups and aromatic structures present in the membrane material. Fig. 1 depicts the spectral

pattern and absorbance intensity of the UF membrane. The absorption bands for the UF membrane spectra were between 800 and 4000 cm^{-1}, which is commonly attributed to the C—H bond of alkene compounds at 836 cm^{-1}. Strong adsorption bands were exhibited at 1098 cm^{-1}, and 1245 cm^{-1}, and these correspond to the aromatic sulfone group and aromatic ether bond, respectively. The other significant peaks were at 1506 cm^{-1}, 1663 cm^{-1}, and 1331 cm^{-1} wavelength, which represent amide group, C—C alkene and carbonyl group respectively [23].

3.2. One Factor at One-Time Approach (OFAT) approach

3.2.1. Effect of filtration time

The normalized flux (the ratio of the permeate flux to the pure water flux, J/J_{pwp}), membrane resistance ratio (the ratio of membrane resistance to the total resistance) are depicted in Fig. 2a and the amount of xylitol produced was demonstrates in Fig. 2b. The filtration process was taken place at 1.2 bar of TMP and 1.06 cm/s of CFV. The flux started to decline when the filtration was initiated, but the ratio of membrane resistance showed the opposite trend with flux decline and thus reduces the amount of xylitol produced which causes fouling. Most possibly, the fouling that has occurred in such cases may be due to the accumulation of enzymes that is xylose reductase on the surface of the membrane or inside its pores. The J/J_{pwp} dropped to 0.63 within 10 min and to 0.45 within 100 min. In comparison, the resistance ratio was increased from 0.58 L/hr.min^2 to 1.03 L/hr.min^2 within 100 min.

Fig. 2a likewise demonstrates the relentless state of permeate flux and hydraulic resistance at 100 min. In this steady-state, the cake layer presumably achieves an equilibrium thickness, while the hydraulic resistance became also constant. During membrane separation, concentration polarization and deposition of gel/cake layer occurred at the surface of the membrane. At the membrane surface, concentration polarization was built up from XR allowing the XR concentration to be greater at the surface of the membrane than in the bulk solution. This results in the accumulation of the cakes, or gel layer at the membrane surface. This cake/gel layer continuous to expand, leading to a reduction in the permeate flux, until the condition become steady state. When the cake layer/gel layer reaches its steady state, the flow of solutes towards the cake layer is equal to the diffusion of solute from the cake layer plus the permeation of solute through membrane [24].

3.2.2. Effect of transmembrane pressure (TMP)

Fig. 3a shows the flux decline as a function of time regardless of various transmembrane pressures (TMP) applied during the xylose reductase separation. Increase in the operational TMP enhances flux declination and thus accelerates the operation to achieve a steady state flux condition. This finding is well supported by the results, which indicate higher operational TMP in higher steady state flux value. This is because of the effect of compaction of gel/cake layer. As the flux increases, more solute mass (XR and reaction mixtures) has been brought to the membrane surface, which increases pore plugging and flow resistance. The later might be a result of the gel/cake layer that resulted in more compact with an increase in transmembrane pressure [25]. It is also worth noting that the gel/cake layer accumulated over the membrane plays an important role in XR separation. In addition, at a higher operational TMP severe decline in flux was observed. The total resistance increases when the TMP is applied, resulting in lower permeate flux, decreased membrane permeability and XR activity during the separation process. High TMP clearly indicates maximal permeate flux but unfortunately it would also increase the rate of membrane fouling, although low TMP decreases the rate of membrane fouling but does not contribute to maximal membrane performance because of its low xylitol mixture concentration [26].

Fig. 3b also shows that the total amount of xylitol produced during separation was found to be linked positively to operational TMP. Thus, increase in the xylitol amount also increases TMP and thus operational TMP in one of the significant parameters that would impact in better XR separation. It is supported by Fig. 3c which depicts that when the TMP increases, the total of xylitol amount also increases at 100-minutes filtration. In addition, high XR separation required high operational TMP in order to maximize the membrane performance. It can be observed from the Fig. 3c, that the constant fouling rates increase when the operational TMP increase from 0.8 bar to 1.2 bar as a function of inverse filtration time. In particular, 1.2 bar of applied TMP resulted in the highest constant fouling rate of 23 % and 24 % than other TMP ranges. Therefore, higher TMP indicates higher degree of initial membrane fouling [20]. To the contrary, Cordovas et al., (2017) investigated three stage series of nanofiltration (NF) of galacto-oligosaccharide (GOS) under critical TMP. An empirical model showed that due to the increase in the solute concentration during batch NF, TMP must be decreased with time to prevent fouling effects. Using NF serial system, the maximum GOS concentration achieved for raw GOS was 241 g/l and 156.8 g/l for pre-hydrolyzed GOS [27].

Table 3
ANOVA tables and summary of fit for membrane permeability.

Source	Sum of Squares	DF	Mean Square	F Value	Prob >F	
Model	121.38	9	13.49	300.00	<0.0001	significant
x_1	17.81	1	17.81	396.11	<0.0001	
x_2	38.25	1	38.25	850.89	<0.0001	
x_3	53.25	1	53.25	1164.32	<0.0001	
x_1x_2	0.031	1	0.031	0.70	0.4239	
x_1x_3	0.051	1	0.051	1.14	0.3110	
x_2x_3	4.81	1	4.81	106.88	<0.0001	
x_1^2	0.072	1	0.072	1.60	0.0032	
x_2^2	4.55	1	4.55	101.12	<0.0001	
x_3^2	1.78	1	1.78	39.58	<0.0001	
Residual	0.45	10	0.045			
Lack of Fit	0.13	5	0.026	0.41	0.8252	not significant
Pure Error	0.32	5	0.064			
Cor Total	121.83	19				
Std.Dev	0.21			R-squared		0.9863
Mean	51.99			Adj R- squared		0.9830
C.V.%	0.41			Pred R-squared		0.9778
Press	1.48			Adeq Precision		66.800

Table 4
ANOVA tables and summary of fit for amount of xylitol produced.

Source	Sum of Squares	DF	Mean Square	F Value	Prob >F	
Model	9.31	9	1.03	46.64	<0.0001	significant
x_1	1.42	1	1.42	64.11	<0.0001	
x_2	2.97	1	2.97	133.76	<0.0001	
x_3	3.68	1	3.68	165.76	<0.0001	
x_1x_2	0.25	1	0.25	11.20	0.0074	
x_1x_3	0.095	1	0.095	4.27	0.0658	
x_2x_3	0.18	1	0.81	8.25	0.0166	
x_1^2	0.031	1	0.031	1.40	0.2645	
x_2^2	0.47	1	0.47	21.08	0.0010	
x_3^2	0.40	1	0.40	18.10	0.0017	
Residual	0.22	10	0.022			
Lack of Fit	0.045	5	9.026E-003	0.26	0.9198	not significant
Pure Error	0.18	5	0.035			
Cor Total	9.53	19				
Std.Dev	0.15	R-squared			0.9767	
Mean	15.56	Adj R- squared			0.9558	
C.V.%	0.96	Pred R-squared			0.9348	
Press	0.62	Adeq Precision			22.944	
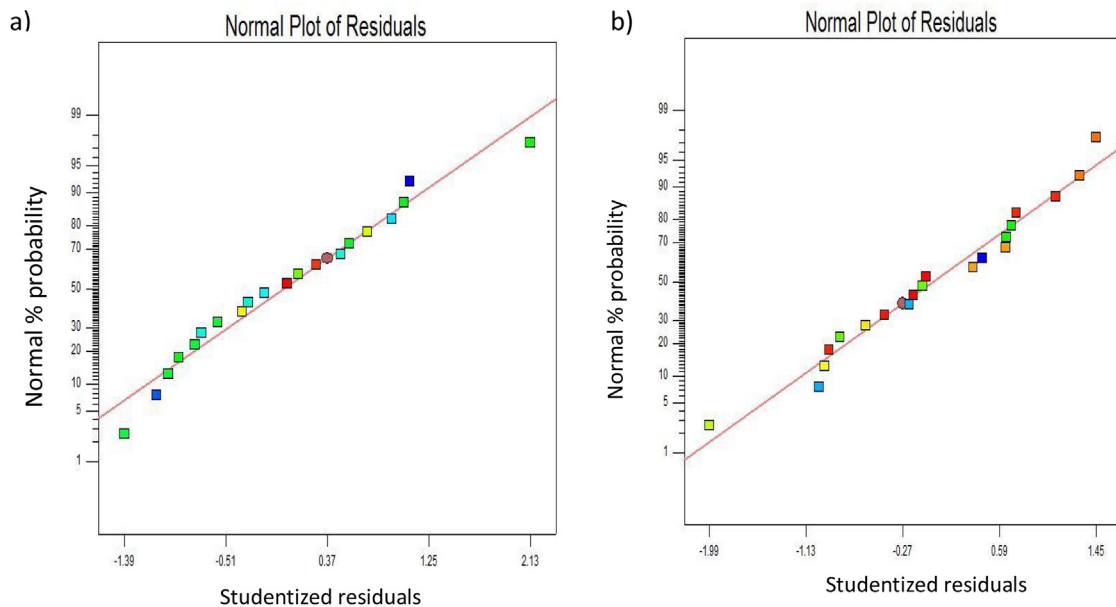
Fig. 6. Normal plot of Residuals response for (a) membrane permeability and (b) amount of xylitol.

3.2.3. Effect of cross flow velocity (CFV)

Cross flow velocity (CFV) is one of the critical parameter that influences membrane separation efficiency. It is a highly important parameter that provides an ideal environment for the separation of xylose reductase, and minimizes the fouling effect. The effects of CFV on the permeate flux and xylitol during filtration is shown in Fig. 4a. The lower CFV (0.58 cm/s) to permeate flux had a noticeable reduced filtration effect as it displayed a greater flux decrease and a higher fouling rate compared to 0.70 cm/s, 0.82 cm/s, 1.06 cm/s and 1.20 cm/s. The lower flux could be related to the compression of fouling layer on the membrane surface at low CFV as a function of filtration time. Later, this fouling layer was considerably found more concentrated as a thick layer. These saturated layers hindered permeate flux through the membrane pores, and generated low reaction mixtures filtrate [28].

Fig. 4a and b indicate that higher CFV implies a higher steady state flux, meaning lesser fouling had occurred on the membrane surface and pores. This finding appears to be consistent with the result obtained in Fig. 4c. This scenario is apparently attributed to the physical scoring effect of CFV on the membrane surface.

Increased CFV resulted in increased shearing stress on the membrane surface, which redistributes the solute particles on the membrane surface. The 1.20 cm/s CFV produced relatively lower fouling later than others ranges, which was then easily removed from the membrane surface by using hydraulic and chemical cleaning. Thus, it is worth noting that high CFV (1.20 cm/s) presumably implied greater membrane for longer operating time without replacing the membrane. In addition, the result of Fig. 4b shows that the amount of xylitol produced was slowly decreased with filtration time irrespective of operating CFV. This scenario is again presumably linked to the deposition of solutes (XR) on the membrane surface and covers all the pores entries, which consequently denoted the flux decline as well as low concentration of xylitol produced. This phenomenon is more critical for 0.58 cm/s of CFV. In short, lesser the CFV, the lesser is the concentration of xylitol produced, and severe is the membrane fouling [21].

Fig. 4c shows the relation between the constant fouling rates with different operations of CFV. The data demonstrated that 1.20 cm/s of CFV exhibits higher constant fouling rates (26 %) compare to the
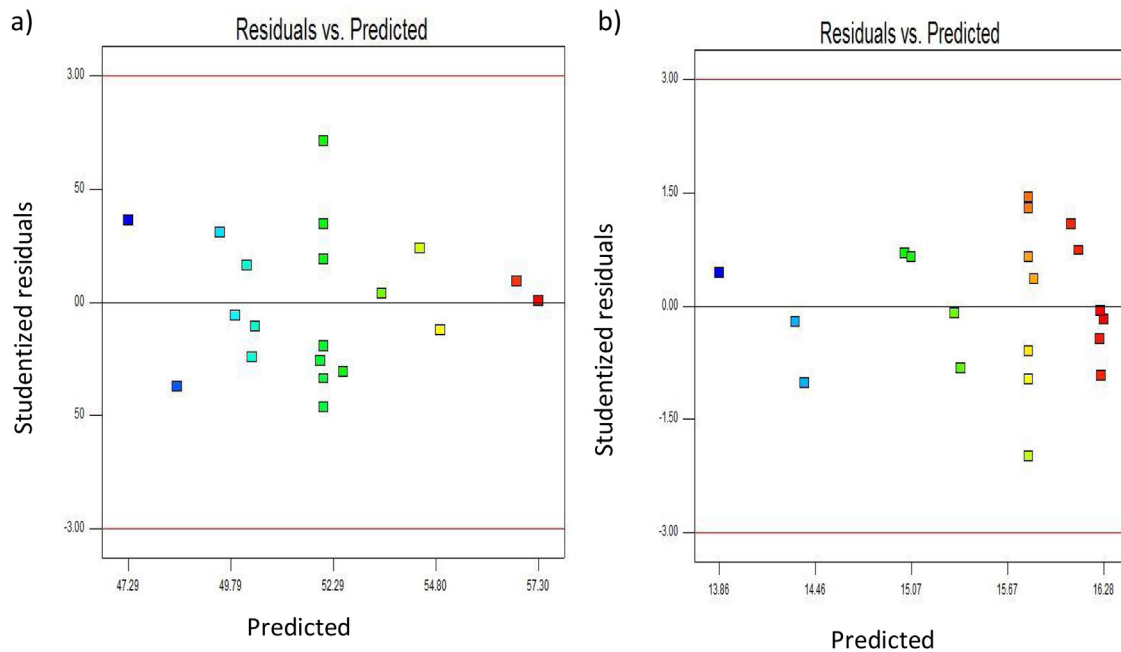
Fig. 7. Plot for residuals vs. predicted response for (a) membrane permeability and (b) amount of xylitol.
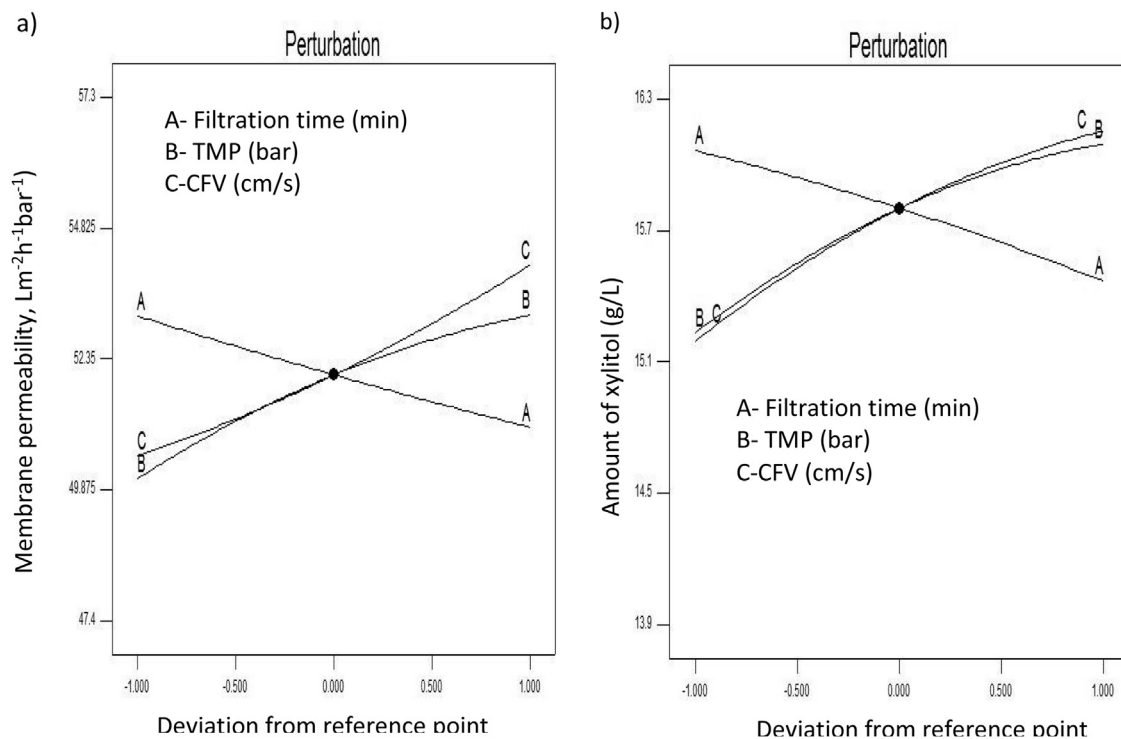

Fig. 8. Perturbation plot indicating, (a) membrane permeability and, (b) amount of xylitol produced with reference to each variable.

other types of CFVs, suggesting higher initial membrane fouling rates. This was evident from higher J_{ss} demonstrated by the high CFV (1.20 cm/s) than the other CFV (0.58, 0.70, 0.82 and 1.06 cm/s). Therefore, the selection of suitable CFV is distinctively essential in XR separation. The high CFV has been revealed to demonstrate lower hydraulic resistance and greater membrane permeability. In this study, the feed was rich in organic solutes (xylose reductase, xylitol, xylose, glucose etc.), and thus this finding supports that alkaline cleaning (using 1 N NaOH) is more suitable in gaining the initial flux.

3.3. Optimization of operating parameters

In order to find the best combination of the operation parameters for the maximum separation of xylose reductase, method of optimization was applied through response surface methodology. The operating parameters involved are represented in Table 1. The experimental plan exhibiting the different combinations of filtration time, cross flow velocity (CFV) and transmembrane pressure (TMP) is tabulated in Table 2. A full factorial central composite design (CCD) involving with 20 runs

Table 5
Results for operating parameters in validation study.

x_1	x_2	x_3	Membrane permeability ($Lm^{-2} h^{-1} bar^{-1}$)			Amount of xylitol (g/L)		
			Actual	Predicted	Error (%)	Actual	Predicted	Error (%)
30.00	1.40	1.06	56.03	57.30	2.21	15.49	16.28	4.85
40.00	1.20	0.88	51.21	52.07	1.65	15.12	15.80	4.30
40.00	1.20	1.24	55.39	56.76	2.41	15.72	16.26	3.32
60.00	1.20	0.88	50.25	50.19	0.12	15.12	15.07	0.33
40.00	1.20	0.88	51.87	52.07	0.39	15.67	15.80	0.83

was carried out with the two given response variables measured was membrane permeability and amount of xylitol produced. The following second order regression equation (Eqs. (4)–(7)) showed the mathematical model in terms of coded and actual factors with respect to membrane permeability and amount of xylitol. Fig. 5 depicts 3D response surfaces to predict the membrane permeability and xylitol amount production over independent variables These equations were optimized by the iteration method using Design Expert 7.1.6.

(4) Membrane permeability, Y_1 (coded):

$$Y_1 = +52.08 - 1.06X_1 + 1.55X_2 + 1.81X_3 - 0.062X_1X_2 - 0.080 X_1X_3 + 0.78\,X_2X_3 + 0.054\,X_1^2 - 0.43\,X_2^2 + 0.27\,X_3^2 \quad (4)$$

(5) Membrane permeability, y_1 (actual):

$$y_1 = +49.75461 - 0.71707x_1 + 15.55044x_2 - 28.45756x_3 - 0.03150\,x_1x_2 - 0.04444\,x_1x_3 + 21.52778\,x_2x_3 + 5.3527E{-}04\,x_1^2 - 10.63068\,x_2^2 + 8.21058\,x_3^2 \quad (5)$$

(6) Amount of xylitol, Y_1 (coded):

$$Y_1 = +15.80 - 0.30\,X_1 + 0.43\,X_2 + 0.48\,X_3 + 0.18X_1X_2 + 0.11 X_1X_3 - 0.15\,X_2X_3 - 0.035\,X_1^2 - 0.14\,X_2^2 - 0.13\,X_3^2 \quad (6)$$

(7) Amount of xylitol, y_1 (actual):

$$y_1 = +5.49626 + 0.16064\,x_1 + 10.50717\,x_2 + 12.15239\,x_3 + 0.088125\,x_1x_2 + 0.060417\,x_1x_3 - 4.20139\,x_2x_3 - 3.51136E{-}004\,x_1^2 - 3.40909\,x_2^2 - 3.90011\,x_3^2 \quad (7)$$

where X_1, X_2, and X_3 are coded forms, while x_1, x_2 and x_3 are actual forms of the best variables as described in Table 2.

According to Eqs. (4) and (5), filtration time (x_1) had the strongest simulation effect on the membrane permeability followed by TMP (x_1) and CFV (x_2). The Eqs. (6) and (7) also depict filtration time had the highest simulation effect on the amount of the xylitol. Based on these results, filtration time provides adverse effects on the membrane permeability and xylitol production as it has a large negative coefficient as indicated by the simulation model equation (Eqs. (4)–(7)). In order to substantiate a good model, an ANOVA table was employed to summarize the test performed.

According to Tables 3 and 4, the values of "Prob > F" for both models were less than 0.0500, which clearly indicate that the model terms are significant. In addition, the main effect of time (x_1), TMP (x_2) and CFV (x_3) are the significant model terms for the membrane permeability response (Table 3) and amount of xylitol (Table 4). The coefficients of determination (R^2) were 0.9863 and 0.9767 for membrane permeability and amount of xylitol produced, respectively. These R^2 values are relatively close to 1.0, which is acceptable. In particular, that the fitted model implies 98.63 % and 97.67 % of total variability in membrane permeability and amount of xylitol.

The predicted R^2 (0.9778 and 0.9348) for membrane permeability and amount of xylitol, respectively) are in reasonable agreement with the adjusted R^2 (0.9830 and 0.9558 for membrane permeability and amount of xylitol, respectively). This values represents the correlation between the experimental values and the predicted values from the model. Furthermore, Tables 3 and 4 reveal that the adequate precision for both responses is greater than 4 (66.800 and 22.944) suggesting adequate model discrimination. The normal probability plot of residuals and the plot of the residuals versus the predicted response are illustrated in Figs. 6 and 7 . The residual points apparently follow straight line and the errors were distributed normally, and thus support adequacy of the least square fit. Fig. 7 exhibits a random scatter which considerably implies that the proposed models are adequate and free from any violation of independence or constant variance assumption.

The perturbation plot (Fig. 8) was plotted out in order to graphically evaluate the effect of each factor (filtration time, TMP, and CFV) for both responses. The perturbation plot describes how these two responses move as the level of the factor changes whilst the other factors are fixed at their optimum levels. Fig. 8 clearly show that each of the three variables employed in this study has its individual effect on the membrane permeability and amount of xylitol produced. Based on the figure below, there has been an increase in the membrane permeability and amount of xylitol produced with an increase in TMP (B) from 1.0 bar (coded value = −1) to 1.4 bar (coded value = +1) and CFV (C) from 0.70 cm/s (coded value = −1) to 1.06 cm/s (coded value = +1). Furthermore, membrane permeability and amount of xylitol has been gradually decreased with an increase in the filtration time (A) from 40 min (coded value = −1) to 80 min (coded value = +1). Thus, the maximum membrane permeability and

Table 6
Summary of optimization operating parameters using experimental design for Separation of xylose reductase from reaction mixtures.

	Before Optimization	After Optimization
Operating parameters:		
Filtration time, min	60min	30min
Transmembrane pressure, bar	1.0 bar	1.4 bar
Cross flow velocity, cm/s	0.88 cm/s	1.06 cm/s
Response:		
Membrane permeability, $Lm^{-2}h^{-1} bar^{-1}$		
• Predicted	49.65	57.30
• Actual		56.03
Amout of xylitol produced, (g/L)		
• Predicted	15.29	16.28
• Actual		15.49

amount of xylitol produced were found to be obtained for the filtration time at 40 min (coded value = −1), TMP at 1.4 bar (coded value = +1) and CFV at 1.06 cm/s (coded value = +1).

3.4. Validation study and confirmation run

Model validation is an important step for the optimization procedures and it is used to verify the acceptability, adequacy and accuracy of the constructed model. In order to validate the reliability of the model, a series of additional experiments were conducted by varying three independent parameters and estimating the resulting membrane permeability and amount of xylitol. Table 5 shows the percentage errors for membrane permeability and amount of xylitol produced ranged from 1.65 % to 2.41 % and from 3.32 % to 4.85 %, respectively. The result indicates that the empirical models developed are noticeably accurate for both membrane permeability and amount of xylitol produced responses. Moreover, the percentage of errors for the actual and predicted values were agreeably within the value of 5 %, suggesting that the model adequacy is reasonably within 95 % of the prediction interval.

In order to confirm the predicted optimization conditions, an experiment was performed using the conditions proposed by the optimization model and the results are demonstrated in the Table 6. Reaction parameters were set to the values defined previously. Under these conditions, the maximum values for membrane permeability and amount of xylitol predicted from the model were 57.30 $Lm^{-2}h^{-1}bar^{-1}$ and 16.28 g/l, respectively. Apparently, the experiment results show that the optimal value of membrane permeability and amount of xylitol filtered were 56.03 $Lm^{-2}h^{-1}bar^{-1}$ and 15.49 g/l, respectively. In short, the percentage error between the actual and predicted value for membrane permeability was 2.21 % while for second response, the percentage error was 4.85 % which both were found to be close to the predicted values and thus, the model was successfully validated. Hence, the optimization of both responses could be achieved by using RSM.

4. Conclusion

The analysis of filtration time, transmembrane pressure (TMP) and crossflow velocity (CFV) for this study can be used for further studies and experiments for optimizing the process for XR separation using an ultrafiltration membrane. FTIR analysis of the membrane reveals the significant peaks were at 1506 cm^{-1}, 1663 cm^{-1} and 1331 cm^{-1} wavelength, which represent amide group, C—C alkene and carbonyl group respectively. Increased transmembrane pressure can lead to a positive effect in flux, since it is the driving force. On the other hand, fouling and polarized layer are more accentuated under higher transmembrane pressure in XR separation. Concurrently, the increasing crossflow velocity was more effective for fouling reduction on the membrane surface. Thus, the best range that could be used for optimization of this process for filtration time, operational transmembrane pressure and cross flow velocity is 30 min, 1.4 bar and 1.06 cm/s, respectively as these conditions yielded the highest membrane permeability and xylitol content. The maximum values for membrane permeability and amount of xylitol predicted from the model were 57.30 $Lm^{-2}h^{-1}bar^{-1}$ and 16.28 g/l, respectively and thus, the model was successfully validated. Further research should be conducted on the scale- up study in determining the suitability of the separation process of XR in industrial applications particularly for the long term usage with the respect to the production of high yield and productivity of xylitol.

CRediT authorship contribution statement

Santhana Krishnan: Writing - original draft, Writing - review & editing, Conceptualization, Data curation, Investigation, Methodology. **B. Noor Suzana:** Formal analysis, Investigation, Resources. **Zularisam Abdul Wahid:** Validation. **Mohd Nasrullah:** Software. **Mimi Sakinah Abdul Munaim:** Supervision. **Mohd Fadhil Bin MD Din:** Visualization. **Shazwin Mat Taib:** Formal analysis. **Yu You Li:** Visualization.

Declaration of Competing Interests

The authors declare that they have no known competing financial interests or personal relationships that could have appeared to influence the work reported in this paper.

Acknowledgements

Appendix A. Supplementary data

Supplementary material related to this article can be found, in the online version, at doi:https://doi.org/10.1016/j.btre.2020.e00498.

References

[1] C. Boi, Membrane chromatography for biomolecule purification, Current Trends and Future Developments on (Bio-) Membranes, (2019) , pp. 151–166.

[2] M. Zhang, A.K. Puri, Z. Wang, S. Singh, K. Permaul, A unique xylose reductase from Thermomyces lanuginosus: effect of lignocellulosic substrates and inhibitors and applicability in lignocellulosic bioconversion, Bioresour. Technol. 281 (2019) 374–381.

[3] J. Meng, Y. Wang, Y. Zhou, J. Chen, X. Wei, R. Ni, F. Xu, Development of different deep eutectic solvent aqueous biphasic systems for the separation of proteins, RSC Adv. 9 (25) (2019) 14116–14125.

[4] C.R. Yolanda, Z.Z. Marisol, L.C.L. Micloth, A.U. MaGuadalupe, Preliminary characteri zation of xylose reductase partially purified by reversed micelles from Candida tropicalis IEC5-ITV, an indigenous xylitol-producing strain, Adv. Chem. Eng. Sci. 2 (2012) 9–14.

[5] C. Borgström, L. Wasserstrom, H. Almqvist, K. Broberg, B. Klein, S. Noack, M.F. Gorwa-Grauslund, Identification of modifications procuring growth on xylose in recombinant Saccharomyces cerevisiae strains carrying the Weimberg pathway, Metab. Eng. 55 (2019) 1–11.

[6] S. Mukherjee, Isolation and purification of industrial enzymes: advances in enzyme technology, Advances in Enzyme Technology, (2019) , pp. 41–70.

[7] J.T. Cunha, P.O. Soares, A. Romaní, J.M. Thevelein, L. Domingues, Xylose fermentation efficiency of industrial Saccharomyces cerevisiae yeast with separate or combined xylose reductase/xylitol dehydrogenase and xylose isomerase pathways, Biotechnol. Biofuels 12 (1) (2019) 20.

[8] M.B. Asif, F.I. Hai, V. Jegatheesan, W.E. Price, L.D. Nghiem, K. Yamamoto, Applications of membrane bioreactors in biotechnology processes, Current Trends and Future Developments on (Bio-) Membranes, (2019) , pp. 223–257.

[9] A. Córdova, C. Astudillo, A. Illanes, Membrane technology for the purification of enzymatically produced oligosaccharides, Sep. Funct. Mol. Food Membr. Technol. 120 (2019) 113–153.

[10] A. Sharma, D.G. Bracewell, Characterisation of porous anodic alumina membranes for ultrafiltration of protein nanoparticles as a size mimic of virus particles, J. Memb. Sci. 580 (2019) 77–91.

[11] S.T. Morthensen, S.B. Sigurdardóttir, A.S. Meyer, H. Jørgensen, M. Pinelo, Separation of xylose and glucose using an integrated membrane system for enzymatic cofactor regeneration and downstream purification, J. Memb. Sci. 523 (2017) 327–335.

[12] P.S. Goh, A.F. Ismail, N. Hilal, Desalination technology and advancement, Oxford Research Encyclopedia of Environmental Science, (2019) .

[13] C. Conidi, E. Drioli, A. Cassano, Membrane-based agro-food production processes for polyphenol separation, purification and concentration, Curr. Opin. Food Sci. 23 (2018) 149–164.

[14] S. Zaccaria, N.A. Boff, F. Bettin, A.J.P. Dillon, Use of micro-and ultrafiltration membranes for concentration of laccase-rich enzymatic extract of Pleurotus

sajor-caju PS-2001 and application in dye decolorization, Chem. Pap. 73 (12) (2019) 3085–3094.

[15] R.K. Dereli, F.P. Van der Zee, I. Ozturk, J.B. van Lier, Treatment of cheese whey by a cross-flow anaerobic membrane bioreactor: biological and filtration performance, Environ. Res. 168 (2019) 109–117.

[16] V.B. Brião, C.R.G. Tavares, Pore blocking mechanism for the recovery of milk solids from dairy wastewater by ultrafiltration, Braz. J. Chem. Eng. 29 (2) (2012) 393–407.

[17] Z. Zhang, J. Peng, C. Srinivasakannan, Z. Zhang, L. Zhang, Y. Fernández, J.A. Menéndez, Leaching zinc from spent catalyst: process optimization using response surface methodology, J. Hazard. Mater. 176 (2010) 1113–1117.

[18] M. Somasundaram, R. Saravanathamizhan, C. Ahmed Basha, V. Nandakumar, S. Nathira Begum, T. Kannadasan, Recovery of copper from scrap printed circuit board: modelling and optimization using response surface methodology, Powder Technol. 266 (2014) 1–6.

[19] N. Shaari, K.S. Kamarudin, Performance of crosslinked sodium alginate/ sulfonated graphene oxide as polymer electrolyte membrane in DMFC application: RSM optimization approach, Int. J. Hydrogen Energy 43 (51) (2018) 22986–23003.

[20] A.W. Zularisam, A.F. Ismail, M.R. Salim, M. Sakinah, H. Ozaki, The effects of natural organic matter (NOM) fractions on fouling characteristics and flux recovery of ultrafiltration membranes, Desalination 212 (1–3) (2007) 191–208.

[21] I.S.M. Rafiqul, A.M.M. Sakinah, A.W. Zularisam, Enzymatic production of bioxylitol from sawdust hydrolysate: screening of process parameters, Appl. Biochem. Biotechnol. 176 (4) (2015) 1071–1083.

[22] H.M. Ibrahim, W.M.W. Yusoff, A.A. Hamid, R.M. Illias, O. Hassan, O. Omar, Optimization of medium for the production of β- cyclodextrin glucanotransferase using Central Composite Design (CCD), Process. Biochem. 40 (2005) 753–758.

[23] J. Chokki, G. Darracq, P. Pölt, J. Baron, H. Gallard, M. Joyeux, B. Teychené, Investigation of Poly (ethersulfone)/polyvinylpyrrolidone ultrafiltration membrane degradation by contact with sodium hypochlorite through FTIR mapping and two-dimensional correlation spectroscopy, Polym. Degrad. Stab. 161 (2019) 131–138.

[24] K.A. Gebru, C. Das, Removal of bovine serum albumin from wastewater using fouling resistant ultrafiltration membranes based on the blends of cellulose acetate, and PVP-TiO2 nanoparticles, J. Environ. Manage. 200 (2017) 283–294.

[25] C. Baldasso, T.C. Barros, I.C. Tessaro, Concentration and purification of whey proteins by ultrafiltration, Desalination. 278 (1–3) (2011) 381–386.

[26] D.J. Miller, S. Kasemset, D.R. Paul, B.D. Freeman, Comparison of membrane fouling at constant flux and constant transmembrane pressure conditions, J. Memb. Sci. 454 (2014) 505–515.

[27] A. Córdova, C. Astudillo, L. Santibañez, A. Cassano, R. Ruby-Figueroa, A. Illanes, Purification of galacto-oligosaccharides (GOS) by three-stage serial nanofiltration units under critical transmembrane pressure conditions, Chem. Eng. Res. Des. 117 (2017) 488–499.

[28] J.C. Overton, A. Weigang, C. Howell, Passive flux recovery in protein-fouled liquid-gated membranes, J. Memb. Sci. 539 (2017) 257–262.